Precise Stark-shift measurements using an electro-optically modulated laser beam

W. A. van Wijngaarden* and J. Li
Department of Physics, York University, 4700 Keele Street, Toronto, Ontario, Canada M3J 1P3
(Received 21 October 1996)

Stark shifts were determined using an electro-optically modulated laser beam. The voltage required for atoms excited by the laser beam in an electric field, to be simultaneously in resonance as atoms excited by a frequency sideband of the laser in a field free region, was measured. The scalar α_0 and tensor α_2 polarizabilities of the cesium $11D$ state were found to be $\alpha_0(11D_{3/2}) = -2694.6 \pm 2.7$, $\alpha_2(11D_{3/2}) = 2107.5 \pm 2.7$, $\alpha_0(11D_{5/2}) = -3379.5 \pm 5.4$, and $\alpha_2(11D_{5/2}) = 4242.1 \pm 11.4$ MHz/(kV/cm)^2. The tensor polarizabilities are the most accurate yet determined for any atomic state. [S1050-2947(97)04204-2]

PACS number(s): 32.60.+i, 32.10.Dk, 39.30.+w, 42.62.Fi

Precise measurements of Stark shifts provide information about polarizabilities of atomic states that are important for describing a number of properties including charge-exchange cross sections, van der Waals constants, and dielectric constants [1]. Accurate Stark-shift data are also desired for applications such as the measurement of electrode spacings [2] and the determination of electric fields in plasmas [3]. A number of methods to measure Stark shifts have been developed and are described in the review articles by Bederson and Miller [4] and van Wijngaarden [5]. The most accurate data have been obtained using narrow linewidth lasers to excite atomic beams. Typically, the laser beam excites the atoms in a field free region and subsequently in a uniform electric field. The frequency difference separating the resonance as observed in the field free and field regions is found by passing part of the laser beam through an interferometer. The accuracy of this method has been typically limited to several percent by temperature and pressure fluctuations, which affect the frequency calibration of the interferometer as well as by scanning nonlinearities of the laser frequency.

Optical modulators permit a much improved determination of frequency shifts. Part of the laser beam passes through the modulator and is frequency shifted. The frequency unshifted laser beam excites the atoms as they pass through the electric field while the frequency shifted laser beam excites the atoms in the field free region. The Stark shift is found by measuring the voltage for a given modulation frequency such that atoms in both the field and field free regions are simultaneously in resonance. Stark shifts of a number of transitions have been measured using an acousto-optic modulator to frequency shift laser beams by less than a few hundred MHz [6–8]. In contrast, electro-optic modulators can generate frequency shifts of many GHz and therefore permit the study of transitions having larger Stark shifts. Measurements can also be taken using higher voltages where potential systematic effects including contact potentials and small residual frequency shifts are less significant. Electro-optic modulators do not spatially deflect the frequency sidebands from the frequency unshifted laser beam unlike acousto-optic modulators. This ensures that the various frequency components of the laser have the identical alignment relative to the atomic beam. If this were not the case, then different residual first-order Doppler shifts occur complicating the task of frequency calibration.

This experiment examined the cesium $6P_{3/2} \rightarrow 11D_{3/2,5/2}$ transitions. Cesium is an alkali atom and can therefore be modeled as consisting of a valence electron that orbits a nucleus surrounded by an inner electron core. The Stark shifts of the cesium D lines have been studied by Tanner and Wieman [6] and by the group of Hunter [7]. The results agree closely with theoretical calculations made by Norcross [9]. The Stark shifts of the $6P_{3/2} \rightarrow (10\text{–}13)S_{1/2}$ transitions have been examined and the polarizabilities of the (10–13) $S_{1/2}$ states agreed with those obtained by a Coulomb approximation calculation to within a few parts in 1000 [8]. The results of the present work for the tensor polarizabilities of the $11D_{3/2,5/2}$ states are ten times more accurate than the best existing measurements for any atomic state. This therefore stringently tests the ability of theory to predict polarizabilities of states having a spin-orbit splitting, which is not considered by the Coulomb approximation.

The cesium $11D$ state is described by the Hamiltonian [10]

$$H - a\mathbf{L}\cdot\mathbf{S} - \left\{ \alpha_0 + \alpha_2 \frac{3L_z^2 - \mathbf{L}^2}{L(2L-1)} \right\} \frac{E^2}{2}, \qquad (1)$$

where the first term represents the spin-orbit interaction where a is the coupling constant that equals 39 GHz, $\mathbf{L}$ is the orbital electronic angular momentum, and $\mathbf{S}$ is the electronic spin. The second term describes the response of the atom to an external electric field $\mathbf{E}$, which defines the quantization axis. α_0 and α_2 are the scalar and tensor polarizabilities of the $11D$ state, respectively. For $L < 1$, the term dependent on α_2 vanishes. The Hamiltonian does not include the hyperfine interaction since the hyperfine splitting of the $11D_{3/2,5/2}$ states is too small to resolve and so are the Stark shifts of the various hyperfine levels of the $6P_{3/2}$ state.

The spin-orbit interaction of the $11D$ state is much larger than the Stark shifts used in this experiment. The eigenstates are approximately given by $|Jm_J\rangle$ where m_J is the azimuthal quantum number corresponding to the total electronic momentum J. The Stark energy shift is given by

*Electronic address: wvw@yorku.ca

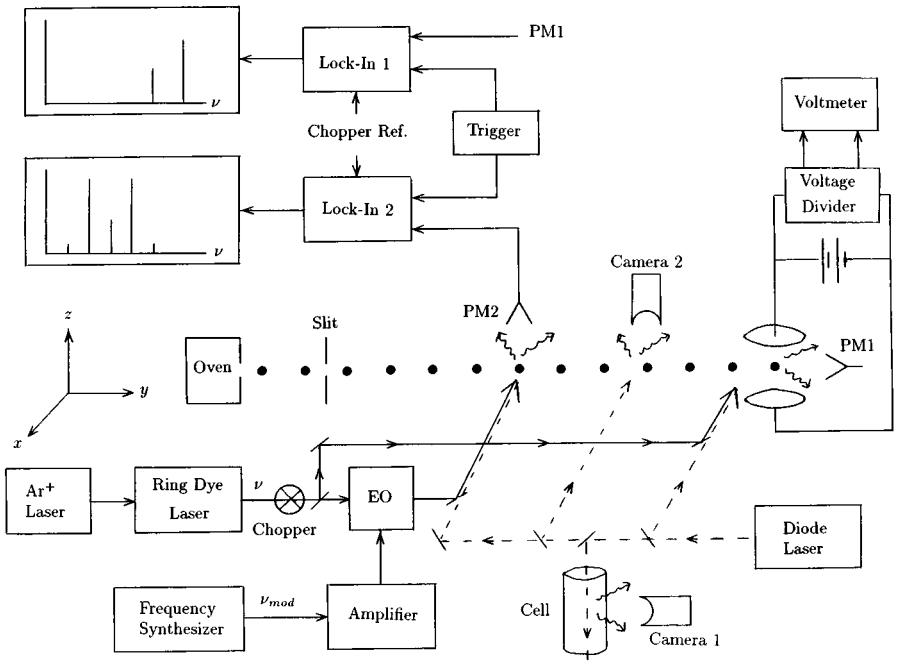

FIG. 1. Apparatus. See text for a detailed discussion.

$$\mathcal{E}=hK\frac{E^2}{2}, \tag{2}$$

where h is Planck's constant and the Stark shift rate K is given as follows [10,11]:

$$K(D_{5/2},|m_J|=1/2)=-\alpha_0(D_{5/2})+\frac{4}{5}\alpha_2(D_{5/2})+\frac{3}{250}\frac{\alpha_2(D_{5/2})^2}{a}E^2,$$

$$K(D_{5/2},|m_J|=3/2)=-\alpha_0(D_{5/2})+\frac{1}{5}\alpha_2(D_{5/2})+\frac{9}{125}\frac{\alpha_2(D_{5/2})^2}{a}E^2,$$

$$K(D_{5/2},|m_J|=5/2)=-\alpha_0(D_{5/2})-\alpha_2(D_{5/2}),$$

$$K(D_{3/2},|m_J|=1/2)=-\alpha_0(D_{3/2})+\alpha_2(D_{3/2})-\frac{6}{245}\frac{\alpha_2(D_{3/2})^2}{a}E^2,$$

$$K(D_{3/2},|m_J|=3/2)=-\alpha_0(D_{3/2})-\alpha_2(D_{3/2})-\frac{36}{245}\frac{\alpha_2(D_{3/2})^2}{a}E^2. \tag{3}$$

The apparatus is illustrated in Fig. 1. An atomic beam was generated by heating cesium metal to a few hundred degrees celsius and using a series of collimating slits. The oven and atomic beam path were enclosed in a vacuum chamber. The ground state was excited to the $6P_{3/2}$ state by a so-called distributed Bragg reflector laser diode (Spectra Diode Labs 5712-H1) which generated up to 100 mW single mode light at 852 nm. The diode laser beam passed through a Pyrex cell, which had been evacuated and loaded with cesium metal and also excited the atomic beam. Fluorescence produced by the radiative decay of the $6P_{3/2}$ state back to the ground state was monitored by two infrared cameras. The fluorescent signals obtained in the cell and atomic beam were observed to remain constant during the experiment.

The $6P_{3/2}\rightarrow 11D_{3/2,5/2}$ transitions were excited using light at 550 nm produced by a ring dye laser (Coherent 699). Part of the dye laser beam passed through an electro-optic modulator (ν-Focus 4421), which could frequency shift over 50% of the incoming light for modulation frequencies in the range of 995 to 1005 MHz. A signal synthesizer (Hewlett-Packard 8647 A) generated the modulation frequency $\nu_{\mathrm{mod}}=1000.000\pm0.001$ MHz. An amplifier increased the power of this signal up to 4 W. The electric field was generated by applying a voltage across two stainless steel plates having a diameter of 12.70 cm and a plate spacing of 2.5395 ± 0.0006 cm. The field was determined using a voltage divider to an accuracy of 0.03%. Fluorescence produced by the radiative decay of the $11D$ state back to the $6P_{3/2}$ state was detected by two photomultipliers. The two resulting signals were processed by separate lock-in amplifiers whose reference signal was provided by a chopper that modulated the laser beam at a frequency of 2 kHz. The lock-in amplifiers digitized the demodulated lock-in signal when externally triggered by a signal generator at a rate of 256 Hz.

The dye laser frequency ν was scanned across the resonance while the fluorescence was recorded as shown in Fig. 2. Figure 2(a) shows the fluorescence signal obtained by exciting the atomic beam in the field free region using the frequency modulated dye laser beam. Five peaks are shown due to excitation of the transition by the components of the laser beam having frequencies ν, $\nu\pm\nu_{\mathrm{mod}}$, and $\nu\pm2\nu_{\mathrm{mod}}$. The laser scan shown took about 2 min and consisted of over 30 000 points. The number of points separating the various 1-GHz intervals was found using several hundred different scans and were found to be consistent with each other, show-

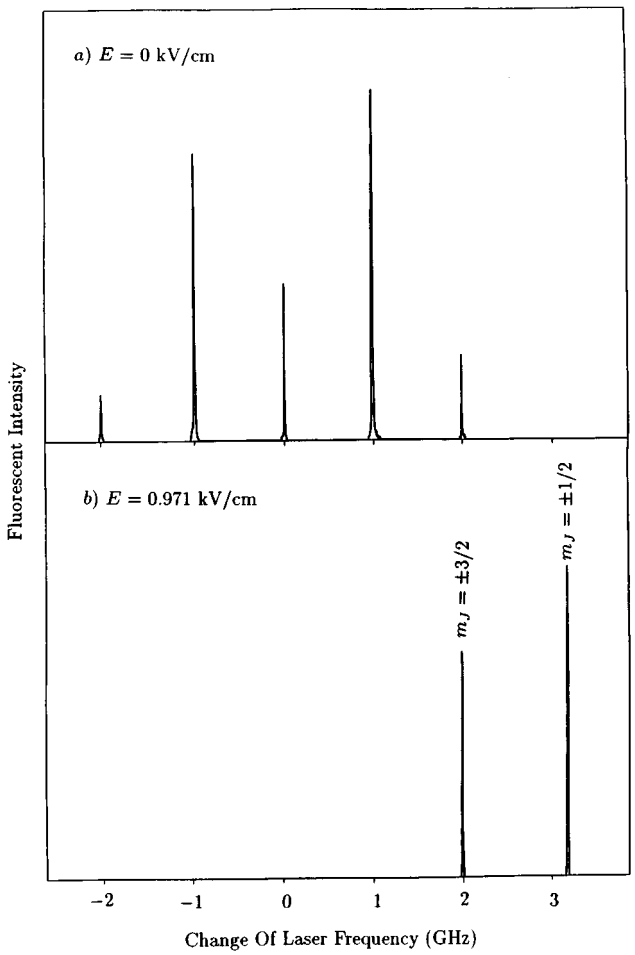

FIG. 2. Fluorescence vs change of laser frequency. (a) shows the fluorescence generated when the frequency modulated laser excited the atomic beam in a field free region. Five peaks corresponding to laser frequency components ν, $\nu \pm \nu_{\mathrm{mod}}$, and $\nu \pm 2\nu_{\mathrm{mod}}$, where $\nu_{\mathrm{mod}} = 1000.000$ MHz, are shown. (b) shows the fluorescence produced when atoms are excited by the laser at frequency ν in an electric field.

ing that the frequency scan is linear to better than 1 part in 1000. Each point was found to correspond to an average value of 0.1898 ± 0.0003 MHz.

Data were first taken without any voltage applied to the electric field plates. The purpose of this was to check whether the atoms in the two regions where the laser intersects the atomic beam were excited by the same laser frequency. A frequency offset ν_{off} occurs if there is a slightly different alignment of the laser beams in the two regions with the atomic beam creating a different residual first order Doppler shift. ν_{off} was measured to have an average value of 7.97 ± 0.45 MHz. One can try to null out this offset by adjusting the beam angles. However, this would not improve the accuracy of the frequency measurement, which is determined by the offset uncertainty.

Data were next taken by applying an electric field across the plates. The dye laser was linearly polarized parallel to the electric field and therefore excited the atoms from the $6P_{3/2}$ state to the $|m_J| = 1/2, 3/2$ levels of the $11D_{3/2,5/2}$ states. Hence, the fluorescence signal shown in Fig. 2(b) shows two peaks. The peak centers were found by the lock-in amplifier, which fitted a Gaussian function to the data as is shown in Fig. 3. The results were found to be independent of voltage polarity and the dye laser power, which was varied by a factor of 100 using neutral density filters. The line shape was broadened at the higher powers but the peak was not frequency shifted. Each dye laser beam was attenuated to a power of less than 1 mW to reduce power broadening while data as shown in Fig. 2 were collected. The measured Stark shifts obtained for the $11D_{3/2}$, $|m_J| = 3/2$ level as a function of electric field squared are shown in Fig. 4. The function $y = (a_1 + a_2 E^2 + a_3 E^4) E^2/2$ was fitted to the data yielding $a_1 = 587.1 \pm 2.9$ MHz/(kV/cm)^2, which from Eqs. (2) and (3) equals $-\alpha_0(11D_{3/2}) - \alpha_2(11D_{3/2})$.

For the $11D_{5/2}$, $|m_J| = 1/2, 3/2$ and $11D_{3/2}$, $|m_J| = 1/2$ levels, the voltage was measured such that the Stark-shifted peak overlapped with the peak excited in the field free region by either the first- or second-order frequency sideband of the laser. The Stark shift of the $11D_{5/2}$, $|m_J| = 5/2$ levels was

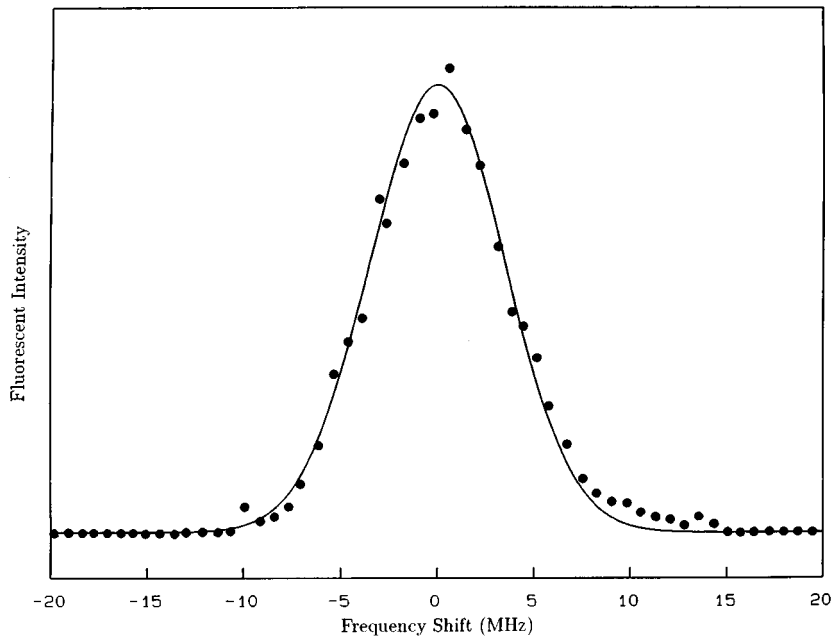

FIG. 3. Example of Gaussian fit to data. The observed FWHM linewidth of 8 MHz is power broadened from the natural linewidth of 5 MHz. This broadening did not affect the determination of the Stark shift as is discussed in the text.

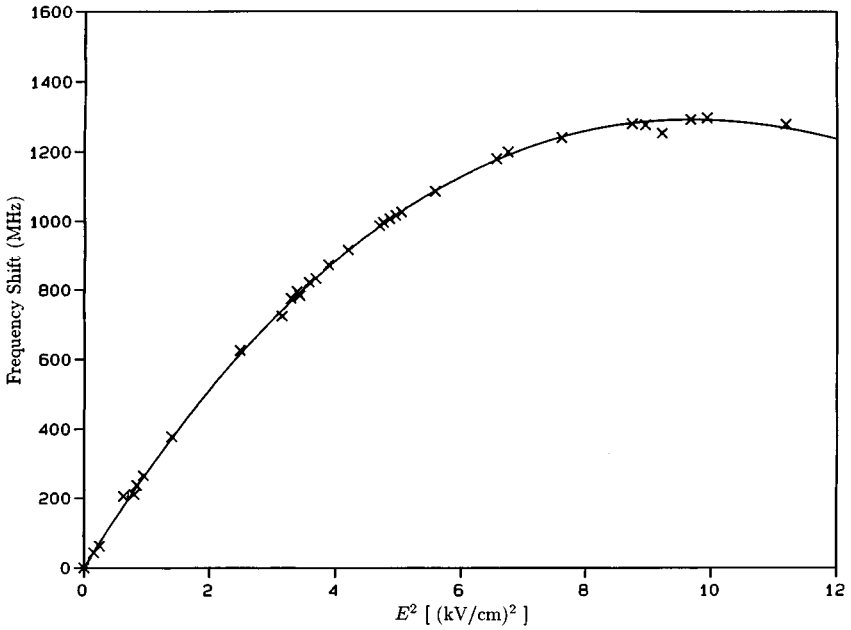

FIG. 4. Frequency shift vs electric field squared for the $11D_{3/2}$, $|m_J|=3/2$ level. The fitted curve is given by $y=293.55E^2-19.4E^4+0.29E^6$, where y is the frequency shift (MHz) and E is the electric field measured in kV/cm.

not studied since this would not yield any additional information about the polarizabilities. These levels can be excited if the dye laser is linearly polarized in the y direction but the fluorescence produced by the decay of the $11D_{5/2}$ state is then primarily emitted in directions where the vacuum chamber blocks viewing. The peak separation was plotted versus the square of the electric field. A least-squares routine fitted a line $y=AE^2+B$ to the data to determine the electric field E_0 corresponding to zero peak separation. The Stark-shift rate obtained by measuring the overlap of the peak excited by the nth-order laser sideband with the peak observed in the electric field region is given by

$$K_0=\frac{n\nu_{\mathrm{mod}}+\nu_{\mathrm{off}}}{E_0^2/2}. \tag{4}$$

Figure 5 shows data taken for the $11D_{5/2,}$ $|m_J|=3/2$ state. Zero peak separation was found to occur at an electric field $E_0=970.82\pm0.42$ V/cm. The quoted uncertainty was found by summing the uncertainties due to statistics, plate geometry, and voltage measurement in quadrature. The resulting Stark shift rate found using Eq. (4) is given in Table I. The scalar and tensor polarizabilities were first estimated using Eq. (3) neglecting the dependence of the Stark shift on E^4. The tensor polarizability was then used to evaluate the term in Eq. (3) proportional to E^4 whose value is labeled as correction in Table I. Finally, the corrected Stark-shift rates were used to determine the polarizabilities given in Table II.

Table II also lists results for the $11D_{5/2}$ state obtained by Fredriksson and Svanberg [11]. They used a rf lamp to excite the $6P_{3/2}$ state and a dye laser having a linewidth of 75 MHz to populate the $11D_{5/2}$ state. Hence, their fluorescent signals

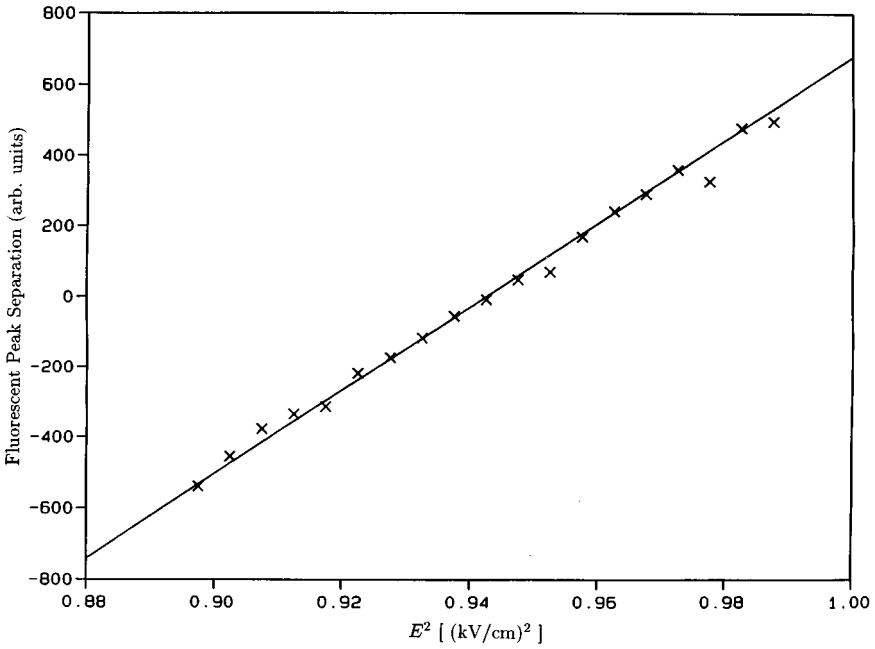

FIG. 5. Fluorescent peak separation vs electric field squared for the $11D_{5/2,}$ $|m_J|=3/2$ level. The frequency difference measured in arbitrary units between the peak produced by the second-order laser sideband at frequency $\nu+2\nu_{\mathrm{mod}}$ in the field free region and the $11D_{5/2}$, $|m_J|=3/2$ peak generated by the laser at frequency ν in the electric field is plotted.

TABLE I. Determination of Stark-shift rate. Units are MHz/(kV/cm)^2.

State	K_0	Correction	K
$11D_{3/2}$, $\|m\|=1/2$	4799.74 ± 4.63	$+2.33\pm0.02$	4802.07 ± 4.63
$11D_{5/2}$, $\|m\|=1/2$	6777.43 ± 5.67	-3.21 ± 0.03	6774.22 ± 5.67
$11D_{5/2}$, $\|m\|=3/2$	4259.62 ± 3.80	-30.66 ± 0.29	4228.96 ± 3.81

had a significantly lower signal-to-noise ratio than the present experiment. An interferometer was used to measure the change in laser frequency and the electric field was determined to an accuracy of a few percent. The data have also been compared to the results of a Coulomb approximation calculation [12]. The close agreement of the theoretical calculation with the experimental results is surprising since the Coulomb potential does not take into account the spin-orbit interaction of the D states.

In conclusion, electro-optic modulators are ideally suited for measuring Stark shifts. The method is not affected by pressure and temperature fluctuations that limit the accuracy of Fabry-Pérot étalons and is relatively insensitive to scanning nonlinearities of the laser. Alignment of the various laser frequency components with the atomic beam is much simpler than in the case of acousto-optic modulators. The data obtained for the polarizabilities of the cesium $11D_{3/2,5/2}$ states are nearly two orders of magnitude more accurate than that obtained previously and the tensor polarizabilities are the most accurate known for any atomic state. Hence, electro-optic modulators have a promising future for studying Stark shifts.

TABLE II. Scalar and tensor polarizabilities in units of MHz/(kV/cm)^2.

State	α_0	α_2	Reference
$11D_{3/2}$	-2694.6 ± 2.7	2107.5 ± 2.7	this work
	-2712	2120	theory [12]
$11D_{5/2}$	-3790 ± 350	4010 ± 400	[11]
	-3379.5 ± 5.4	4242.1 ± 11.4	this work
	-3384	4255	theory [12]

The authors wish to thank the Natural Science and Engineering Research Council of Canada for financial support.

[1] K. D. Bonin and M. A. Kadar-Kallen, Phys. Rev. A **47**, 944 (1993).
[2] C. Neureiter, R. H. Rinkleff, and L. Windholz, J. Phys. B **19**, 2227 (1986).
[3] J. E. Lawler and D. A. Doughty, Adv. At. Mol. Opt. Phys. **34**, 171 (1995).
[4] T. M. Miller and B. Bederson, Adv. At. Mol. Opt. Phys. **25**, 37 (1988).
[5] W. A. van Wijngaarden, Adv. At. Mol. Opt. Phys. **36**, 141 (1996).
[6] C. E. Tanner and C. Wieman, Phys. Rev. A **38**, 162 (1988).
[7] L. R. Hunter *et al.*, Opt. Commun. **94**, 210 (1992).
[8] W. A. van Wijngaarden *et al.*, Phys. Rev. A **49**, R2220 (1994).
[9] H. L. Zhou and D. W. Norcross, Phys. Rev. A **40**, 5048 (1989).
[10] A. Khadjavi, A. Lurio, and W. Happer, Phys. Rev. **167**, 128 (1968).
[11] K. Fredriksson and S. Svanberg, Z. Phys. A **281**, 189 (1977).
[12] W. A. van Wijngaarden and J. Li, J. Quant. Spectrosc. Radiat. Transfer **52**, 555 (1994).